

Updated Constraints from B Physics on the MSSM and the NMSSM

Florian Domingo* and Ulrich Ellwanger†

Laboratoire de Physique Théorique‡

Université de Paris XI, F-91405 Orsay Cedex, France

Abstract

We update constraints from B physics observables on the parameters of the MSSM and the NMSSM, combining them with LEP constraints. Presently available SM and Susy radiative corrections are included in the calculations, which will be made public in the form of a Fortran code. Results for the $\tan\beta$ and M_{H^\pm} dependence of $BR(\bar{B} \rightarrow X_s \gamma)$ are presented, as well as constraints on the NMSSM specific case of a light CP odd Higgs scalar. We find that the latter are essentially due to $BR(\bar{B}_s \rightarrow \mu^+ \mu^-)$, but they do not exclude this possibility.

*email: domingo@th.u-psud.fr

†email: ellwanger@th.u-psud.fr

‡Unité mixte de Recherche – CNRS – UMR 8627

1 Introduction

It is well known that rare decays and/or oscillations of B -Mesons impose constraints on the parameter space of models Beyond the Standard Model (BSM): BSM contributions are not necessarily suppressed, once the dominant contributions both in the SM and BSM arise from loop diagrams (or are even absent in the SM).

Recently, considerable progress has been made both on the experimental side (such as improved measurements of small branching ratios) and on the theoretical side, i.e. improved evaluations of SM predictions and BSM contributions.

The purpose of the present paper is to study the resulting constraints on the parameter space of supersymmetric extensions of the standard model, both in the MSSM and the NMSSM, from $BR(\bar{B} \rightarrow X_s \gamma)$, ΔM_s , ΔM_d , $BR(\bar{B}_s \rightarrow \mu^+ \mu^-)$ and $BR(\bar{B}^+ \rightarrow \tau^+ \nu_\tau)$. In the MSSM, similar analyses have recently been performed in [1–4] (see also refs. [5–10] for recent discussions within the Minimal Flavour Violating MSSM).

In [1, 2] the new experimental B physics results have been used to constrain the parameter space of the MSSM. In [3] it has been argued, that the new results on $BR(\bar{B}^+ \rightarrow \tau^+ \nu_\tau)$ are evidence for BSM contributions. A general χ^2 fit has been performed in [4] in the context of the CMSSM (with universal Susy-breaking terms at the GUT scale) and the NUHM (with non-universal Higgs mass terms), together with constraints on the dark matter relic density.

One purpose of the present paper is to consider constraints from $BR(\bar{B} \rightarrow X_s \gamma)$ on the NMSSM. Our result is that the NMSSM specific effects on $BR(\bar{B} \rightarrow X_s \gamma)$ are rather weak: in the NMSSM the charged Higgs mass squared receives (at tree level) a negative contribution relative to the MSSM which lowers its mass somewhat; once the result of $BR(\bar{B} \rightarrow X_s \gamma)$ is plotted against M_{H^\pm} , no difference between the MSSM and the NMSSM remains visible, however. Two loop corrections (relevant at large $\tan \beta$) are sensitive to the neutralino sector which includes the singlino in the NMSSM; we find, however, that even for relatively large singlino – MSSM-like-neutralino mixings the NMSSM specific numerical effect on $BR(\bar{B} \rightarrow X_s \gamma)$ is numerically negligible. (Combined constraints on the parameter space of the NMSSM from LEP, the dark matter relic density and B physics – but without the recent developments in B physics – have been investigated previously in [11, 12].)

Note that in the general MSSM, LEP constraints on the lightest Higgs mass impose $\tan \beta \gtrsim 3$ (or $\tan \beta \gtrsim 10$ in the CMSSM). In the NMSSM (and the CNMSSM), LEP constraints on Higgs masses and couplings allow for rather low values of $\tan \beta$ [13, 14]; here $\tan \beta$ can be as low as 1.5. Our results for $BR(\bar{B} \rightarrow X_s \gamma)$ for low values of $\tan \beta$ (which have not been considered in [1–4]) are thus specific to the NMSSM, although the results in

the MSSM (without LEP constraints) would have been the same.

In the NMSSM, important new contributions to B physics observables can originate from the presence of a relatively light CP odd Higgs boson [15–22], which can also be consistent with the dark matter relic density [11, 12], and which can contribute significantly via s-channel single and double penguin diagrams to B physics processes even for small $\tan\beta$. Constraints from B physics observables on this region of the parameter space of the NMSSM will be discussed in section 5.

Our numerical results are obtained with the help of a Fortran code, that will be made public as a part of the NMSSMTools package [23]. It allows us to combine the constraints on the parameter space from B physics with constraints on the Higgs sector from LEP. (In the MSSM, subroutines that compute B physics observables are included in FeynHiggs [24], Suspect [25], MicrOmegas [26, 27] and Spheno [28]. Once all the calculations described below are included in NMSSMTools, it can also be used for the MSSM, since the MSSM is just a particular limiting case of the NMSSM.)

In the remaining part of the introduction we briefly review the experimental and theoretical status of the various B physics observables, which are considered in the present paper.

In the past constraints from $b \rightarrow s\gamma$ have been particularly severe, since the experimental world average for $BR(\bar{B} \rightarrow X_s\gamma)$ was somewhat below the (NLO) SM prediction [29, 30], whereas at least the contribution involving a charged Higgs boson in the relevant diagram is positive.

This situation has changed considerably during the last years: the present world average estimated by the Heavy Flavour Averaging Group [31] reads (for $E_\gamma > E_0 = 1.6$ GeV)

$$BR(\bar{B} \rightarrow X_s\gamma)\Big|_{exp} = (3.55 \pm 0.24_{-0.10}^{+0.09} \pm 0.03) \times 10^{-4}. \quad (1.1)$$

The SM NNLO ($\mathcal{O}(\alpha_s^2)$) corrections to the total $BR(\bar{B} \rightarrow X_s\gamma)$ branching fraction have recently be combined [32, 33], which give

$$BR(\bar{B} \rightarrow X_s\gamma)\Big|_{SM} = (3.15 \pm 0.23) \times 10^{-4}. \quad (1.2)$$

In [34] the treatment of the cut $E_\gamma > 1.6$ GeV on the photon energy has been improved, leading to a still lower SM prediction:

$$BR(\bar{B} \rightarrow X_s\gamma)\Big|_{SM} = (2.98 \pm 0.26) \times 10^{-4}. \quad (1.3)$$

This result can be interpreted as (still weak) evidence for BSM contributions to $b \rightarrow s\gamma$; in any case constraints on the parameter space of Susy models have become considerably less stringent.

Next we turn to $\Delta M_{s,d}$. ΔM_s has recently been measured by the CDF collaboration [35] with the result

$$\Delta M_s^{exp} = 17.77 \pm .12 \text{ ps}^{-1} . \quad (1.4)$$

A standard model prediction

$$\Delta M_s^{SM} = 20.5 \pm 3.1 \text{ ps}^{-1} \quad (1.5)$$

can be obtained using a determination of $|V_{ts}^* V_{tb}| = (41.3 \pm .7) \times 10^{-3}$ from tree level processes (where effects from BSM physics affect the higher order corrections only) [6], and a determination of $f_{B_s} \sqrt{\hat{B}_{B_s}} = 0.281 \pm .021 \text{ GeV}$ by the HPQCD collaboration [36]. (In [36], the central value $\Delta M_s^{SM} = 20.3 \text{ ps}^{-1}$ has been obtained, since $|V_{ts}^* V_{tb}| = 41.0 \times 10^{-3}$ has been used. We note that here and below the CKM matrix elements are defined in terms of a low energy effective Lagrangian, whose parameters are determined from low energy processes [37]. In [37], these CKM matrix elements are denoted by V_{eff} , but we omit the subscript "eff" in the following.) Hence, a negative contribution to ΔM_s from BSM processes would be welcome.

ΔM_d is quite well known [31],

$$\Delta M_d^{exp} = 0.507 \pm .004 \text{ ps}^{-1} . \quad (1.6)$$

Again, a standard model prediction (see also [8])

$$\Delta M_d^{SM} = 0.59 \pm 0.19 \text{ ps}^{-1} \quad (1.7)$$

can be obtained using a determination of $|V_{td}^* V_{tb}| = (8.6 \pm 1.4) \times 10^{-3}$ from tree level processes [6], $f_{B_s} \sqrt{\hat{B}_{B_s}}$ as above, and $f_{B_s} \sqrt{\hat{B}_{B_s}} / f_{B_d} \sqrt{\hat{B}_{B_d}} = 1.216 \pm .041$ from [38].

The various Susy diagrams which contribute to ΔM_q ($q = s, d$) are box diagrams involving charged Higgs bosons, stops and charginos (see, e.g., [39]), and double penguin diagrams involving neutral CP even or CP odd Higgs bosons whose contributions increase like $\tan^4 \beta$ for large $\tan \beta$ (see [37] for a detailed analysis). As a function of the mass M_H of the Higgs boson, these contributions to the Wilson coefficients behave like $1/M_H^2$, and depend on the mixing angles of the CP even and CP odd Higgs mass matrices. In the MSSM, the dominant contributions $\sim 1/M_h^2$ (where h denotes the lightest Higgs scalar) cancel at large $\tan \beta$ [37], and one is left with contributions $\sim 1/M_A^2$ (where A denotes the CP odd scalar in the MSSM, whose mass is close to the heavy CP even scalar for large M_A) which cannot be too large, given the lower bound on M_A in the MSSM.

In the NMSSM, three neutral CP even and two CP odd Higgs bosons (we neglect the Goldstone boson here) contribute to the double penguin diagrams. Notably the lightest

CP odd Higgs boson A_1 can be quite light in the NMSSM and escape the present LEP constraints [15–21], but with couplings strong enough to generate large effects for low M_{A_1} [17]. Interestingly, the resulting contributions to ΔM_s are negative which can improve the agreement with its measurement.

Neutral Higgs bosons with effective flavour violating couplings contribute also to $BR(\bar{B}_s \rightarrow \mu^+\mu^-)$, where the new CDF result is at 95% confidence level [40]

$$BR(\bar{B}_s \rightarrow \mu^+\mu^-)\Big|_{exp} < 5.8 \times 10^{-8} . \quad (1.8)$$

(At present, constraints from $BR(\bar{B}_d \rightarrow \mu^+\mu^-)$ are less restrictive.) The SM prediction is still smaller by an order of magnitude [41, 42],

$$BR(\bar{B}_s \rightarrow \mu^+\mu^-)\Big|_{SM} = (3.8 \pm 0.1) \times 10^{-9} , \quad (1.9)$$

which leaves some room for BSM contributions. Again, a light CP odd Higgs boson A_1 can lead to an important effect in the NMSSM [17]; in the case of $BR(\bar{B}_s \rightarrow \mu^+\mu^-)$, however, its contribution must not be too large.

Finally we turn to $BR(\bar{B}^+ \rightarrow \tau^+\nu_\tau)$, which has been observed by the Belle [43] and BABAR [44] experiments. The actual world average performed by the Heavy Flavor Averaging Group [31] is

$$BR(\bar{B}^+ \rightarrow \tau^+\nu_\tau)\Big|_{exp} = (1.32 \pm .49) \times 10^{-4} . \quad (1.10)$$

Unfortunately, the corresponding SM prediction is handicapped by a large uncertainty concerning the CKM matrix element $|V_{ub}|$ [31, 45]: Its determination from inclusive semileptonic b decays gives values near $|V_{ub}| \sim 4.4 \times 10^{-3}$, whereas its determination from exclusive semileptonic decays gives values near $|V_{ub}| \sim 3.7 \times 10^{-3}$ (leading to a discrepancy of the order of 2σ). Accordingly, together with the uncertainties from the hadronic parameter f_B , quite different SM predictions for $BR(\bar{B}^+ \rightarrow \tau^+\nu_\tau)$ can be obtained, ranging from $BR(\bar{B}^+ \rightarrow \tau^+\nu_\tau)\Big|_{SM} = (0.85 \pm .13) \times 10^{-4}$ [1] to $BR(\bar{B}^+ \rightarrow \tau^+\nu_\tau)\Big|_{SM} = (1.59 \pm .40) \times 10^{-4}$ [3]. Hence we will allow for quite large theoretical error bars on this process with the result that it hardly constrains the Susy parameter space; this situation can change in the future, however.

In section 2 we describe the sources of the contributions to $BR(\bar{B} \rightarrow X_s\gamma)$ that we take into account. In section 3 we give the sources of our calculations of ΔM_s , ΔM_d , $BR(\bar{B}_s \rightarrow \mu^+\mu^-)$ and $BR(\bar{B}^+ \rightarrow \tau^+\nu_\tau)$. In section 4 we present results for $BR(\bar{B} \rightarrow X_s\gamma)$ both for large $\tan\beta$ (relevant for the MSSM and the NMSSM) and for low $\tan\beta$ (relevant for the NMSSM only).

Finally, in section 5, we investigate combined constraints from $BR(\bar{B} \rightarrow X_s \gamma)$, $\Delta M_{s,d}$, $BR(\bar{B}_s \rightarrow \mu^+ \mu^-)$ and $BR(\bar{B}^+ \rightarrow \tau^+ \nu_\tau)$ in parameter regions relevant simultaneously for the MSSM and the NMSSM, and also on the NMSSM specific region involving a light CP odd Higgs scalar. In all cases we include constraints on the parameter space from LEP on Higgs masses and couplings as in the updated version of NMHDECAY [46, 47]. In section 6 we conclude with a summary and an outlook.

2 Computation of $BR(\bar{B} \rightarrow X_s \gamma)$

The starting point of our computation is the expression for the branching ratio as in [29, 30],

$$BR(\bar{B} \rightarrow X_s \gamma)_{E_\gamma > E_0}^{\Psi, \Psi' \text{ subtracted}} = BR(\bar{B} \rightarrow X_c e \bar{\nu}) \Big|_{exp} \left| \frac{V_{ts}^* V_{tb}}{V_{cb}} \right|^2 \frac{6\alpha_{em}}{\pi C} \left[|K_c + r(\mu_0) K_t + \epsilon_{ew}|^2 + B(E_0) + N(E_0) \right], \quad (2.1)$$

valid for a matching scale $\mu_0 = m_t(m_t)^{\overline{MS}}$.

In (2.1), we use [33]

$$BR(\bar{B} \rightarrow X_c e \bar{\nu}) \Big|_{exp} = 0.1061, \quad (2.2)$$

and

$$\left| \frac{V_{ts}^* V_{tb}}{V_{cb}} \right|^2 = 0.967 \quad (2.3)$$

from tree level processes [6].

C in (2.1) is given by

$$C = \left| \frac{V_{ub}}{V_{cb}} \right|^2 \frac{\Gamma[\bar{B} \rightarrow X_c e \bar{\nu}]}{\Gamma[\bar{B} \rightarrow X_u e \bar{\nu}]} \quad (2.4)$$

for which we use the numerical value [33]

$$C = 0.580. \quad (2.5)$$

E_0 is the lower cutoff on the photon energy, for which we chose $E_0 = 1.6$ GeV. K_t includes the SM top quark and the BSM contributions, whereas K_c denotes the SM charm quark contribution. $r(\mu_0)$ is the ratio $m_b^{\overline{MS}}(\mu_0)/m_b^{1S}$, for which we use [29, 30]

$$r(\mu_0) = 0.578 \left(\frac{\alpha_s(M_Z)}{0.1185} \right) \left(\frac{m_b^{1S}}{4.69} \right)^{0.23} \left(\frac{m_c(m_c)}{1.25} \right)^{-0.003} \left(\frac{\mu_0}{165} \right)^{-0.08} \left(\frac{\mu_b}{4.69} \right)^{0.006} \quad (2.6)$$

with $m_b^{1S} = 4.68$ GeV as in [33] and $\mu_b = m_b(m_b)$. (The dependence on the scale μ_b is in fact negligibly small.)

In (2.1) ϵ_{ew} denotes the electroweak radiative corrections, $B(E_0)$ the (gluon) bremsstrahlung corrections, and $N(E_0)$ are nonperturbative corrections.

Strictly speaking, the expression (2.1) is valid to NLO, where the charm quark contribution (K_c) can be separated from the top quark/BSM contribution (K_t). K_c depends on the ratio m_c/m_b , and hence on the scheme and the scale at which these masses are taken. On the one hand this ambiguity is a NNLO effect, which is responsible for the largest part of the theoretical error in the NLO result [30]

$$BR(\bar{B} \rightarrow X_s \gamma) \Big|^{NLO} = (3.61_{-0.40}^{+0.24} \Big|_{m_c/m_b} \pm .02_{CKM} \pm 0.24_{param.} \pm 0.14_{scale}) \times 10^{-4}. \quad (2.7)$$

We found that the NNLO result (1.2) is reproduced (for $m_{t,pole} = 171.4$ GeV, as assumed in [32, 33]), if one uses the relatively large value

$$\frac{m_c}{m_b} = 0.307 \quad (2.8)$$

(close to the pole quark masses) in the expression for K_c . We believe that as long as the BSM contributions – which are added linearly to the SM contributions in the factor K_t – are not evaluated to NNLO, the error arising from this procedure is not larger than the error intrinsic to the BSM contributions (which is estimated quite conservatively below). It is guaranteed, in any case, that the result for the $BR(\bar{B} \rightarrow X_s \gamma)$ in the decoupling limit of the BSM contributions assumes the NNLO SM value in (1.2).

Subsequently we describe the origin of the formulas used for our evaluation of the quantities K_c , $N(E_0)$, $B(E_0)$, ϵ_{ew} and K_t in (2.1). First, K_c is computed as in Eq. (3.7) in [29], with $\mu_b = m_b$, the value (2.8) for m_c/m_b and

$$\mu_0 = m_t(m_t)^{\overline{MS}} \quad (2.9)$$

for the matching scale μ_0 . The ratio of CKM matrix elements ϵ_s , that appears in Eq. (3.7) in [29], is taken from [33]:

$$\epsilon_s \equiv V_{us}^* V_{ub} / (V_{ts}^* V_{tb}) = -0.011 + i 0.0180 \quad (2.10)$$

The nonperturbative corrections $N(E_0)$ are computed as in Eq. (3.10) in [29] in terms of the lowest order coefficients $K_c^{(0)}$ and $K_t^{(0)}$ (including the BSM contributions to the latter), with $\lambda_2 = 0.12$ GeV². ($N(E_0)$ is actually independent from E_0 in this approximation).

The bremsstrahlung corrections $B(E_0)$ are taken from the appendix E in [29] with, we repeat, an energy cutoff $E_0 = 1.6$ GeV. For the parameter $z = (m_c/m_b)^2$ we use a value consistent with eq. (2.8) above. (In any case the dependence of $B(E_0)$ on z is weak [29].)

The corrections $\sim \epsilon_q$ (with $q = s$) as in Eq. (28) in [30] are taken into account, with ϵ_s given in Eq. (2.10) above. The contributions to $B(E_0)$ from the coefficients $C_i^{(0)}$ with $i = 3 \dots 6$ are neglected as in [29], on the other hand the BSM contributions to the coefficients $C_7^{(0)}$ and $C_8^{(0)}$ are taken into account.

For the electroweak corrections ϵ_{ew} in (2.1) we use the formula (3.9) in [29] (see also Eq. (27) in [30]), which gives a SM contribution $\epsilon_{ew}^{SM} = 0.0071$ according to [48]. To this SM value for ϵ_{ew} we add the BSM contributions as in [29, 30] in terms of the BSM contributions to the coefficients $C_{7,8}$ discussed below.

Finally we turn to the calculation of K_t including the BSM contributions. First, the SM contributions to K_t (including the NLO in α_s) are taken from Eq. (3.8) in [29], with the above Eq. (2.9) for the matching scale μ_0 . The BSM contributions are added as in Eq. (5.1) in [29]. The BSM contributions appear in the LO Wilson coefficients $C_7^{(0)BSM}(\mu_0)$, $C_8^{(0)BSM}(\mu_0)$ and the NLO Wilson coefficients $C_7^{(1)BSM}(\mu_0)$, $C_8^{(1)BSM}(\mu_0)$ and $C_4^{(1)BSM}(\mu_0)$ of the corresponding operators P_i .

Our calculation of these Wilson coefficients within the MSSM and the NMSSM starts with the calculation of the corrections ϵ_b , ϵ'_b and ϵ'_t to the couplings of the charged Higgs bosons to quarks defined in [49] (see also [50]), which are important at large $\tan\beta$. We use the expressions for these parameters given in [27], which include sbottom and electroweak contributions, and in which a sign error in [49] is corrected. In the case of ϵ'_b and ϵ'_t we sum over the 5 neutralino states of the NMSSM with its corresponding masses and couplings. (In the MSSM limit $\lambda, \kappa \rightarrow 0$ of the NMSSM, the fifth neutralino decouples and does not contribute.) Then we proceed with the computation of the following BSM contributions to the Wilson coefficients:

a) The chargino-squark loop contributions to $C_7^{(0)}$ and $C_8^{(0)}$ (as, e.g., in appendix B in [27]), computed again at M_{Susy} and evolved to our matching scale μ_0 . Corresponding NLO corrections are known in the particular case where one stop is lighter than the other squarks and the gluino [51], and the complete QCD corrections have been computed in [52], but here we content ourselves with the summation of the leading logarithms of the ratio M_{Susy}/μ_0 via the RG evolution of the Wilson coefficients.

b) The charged Higgs-top-quark loop contributions to $C_7^{(0)}$ and $C_8^{(0)}$ (again as in appendix B in [27]), and the corresponding NLO contributions to $C_4^{(1)}$, $C_7^{(1)}$ and $C_8^{(1)}$ [53]. The LO contributions to $C_7^{(0)}$ and $C_8^{(0)}$ are evolved from the scale corresponding to the charged Higgs mass to our matching scale μ_0 , and we took care not to include large logarithms – that appear potentially also in the NLO contributions – twice. (Higher order large $\tan\beta$ corrections to the NLO contributions are neglected.)

c) As in [54] we take the neutral Higgs contributions to the Wilson coefficients $C_7^{(0)}$ and $C_8^{(0)}$ into account following Eq. (6.61) in [37]. However, contrary to ΔM_q and $BR(\bar{B}_s \rightarrow \mu^+ \mu^-)$ below, these neutral Higgs effects remain small and usually inside our theoretical error bars.

d) Finally the large $\tan\beta$ corrections induce also a shift in the SM contributions to the coefficients $C_7^{(0)}(\mu_0)$ and $C_8^{(0)}(\mu_0)$ [27, 53].

Herewith we have described completely the origins of the considered contributions to $BR(\bar{B} \rightarrow X_s \gamma)$.

3 ΔM_q , $BR(\bar{B}_s \rightarrow \mu^+ \mu^-)$ and $BR(\bar{B}^+ \rightarrow \tau^+ \nu_\tau)$

In this section, we discuss the sources for our evaluation of the B physics observables ΔM_q ($q = s, d$), $BR(\bar{B}_s \rightarrow \mu^+ \mu^-)$ and $BR(\bar{B}^+ \rightarrow \tau^+ \nu_\tau)$. The formula for ΔM_q is taken from [37], eqs. (6.6–7):

$$\Delta M_q = \frac{G_F^2 M_W^2}{6\pi^2} M_{B_q} \eta_B f_{B_q}^2 \hat{B}_{B_q} |V_{tq}^* V_{tb}|^2 |F_{tt}^q| \quad (3.1)$$

with

$$F_{tt}^q = S_0(x_t) + \frac{1}{4r} C_{new}^{VLL} + \bar{P}_1^{SLL} (C_1^{SLL} + C_1^{SRR}) + \bar{P}_2^{LR} C_2^{LR} + \dots \quad (3.2)$$

where we have omitted negligibly small contributions, and where we take [37] $r = 0.985$, $\bar{P}_1^{SLL} = -0.37$, $\bar{P}_2^{LR} = 0.90$ and $\eta_B = 0.551$. We use the meson masses $M_{B_d} = 5.2794$ GeV and $M_{B_s} = 5.3675$ GeV, and the hadronic parameters $f_{B_s} \sqrt{\hat{B}_{B_s}} = 0.281$ GeV from [36] and $f_{B_d} \sqrt{\hat{B}_{B_d}} = 0.231$ GeV from $f_{B_s} \sqrt{\hat{B}_{B_s}} / f_{B_d} \sqrt{\hat{B}_{B_d}} = 1.216$ [38]. As stated in the introduction, we use the CKM factors deduced from tree level processes, which are less sensitive to BSM physics: $|V_{ts}^* V_{tb}| = 41.3 \times 10^{-3}$ and $|V_{td}^* V_{tb}| = 8.6 \times 10^{-3}$ [6]. S_0 in F_{tt} stands for the SM contribution ($x_t \equiv \left(\frac{m_t^2}{M_W^2}\right)^2$), whereas the coefficients $C_{1,2}^i$ contain BSM contributions to the corresponding effective 4-quark operators.

Let us discuss the various contributions to F_{tt}^q which we take into account (we repeat that we assume minimal flavor violation such that the only source of flavor violation is the CKM matrix): The SM contribution originates from quark/ W^\pm box diagrams. In multi-Higgs extensions of the SM such as the MSSM or the NMSSM, charged Higgs bosons can replace one or both W^\pm bosons in these box diagrams. A second type of box diagrams arises in Susy from squark/chargino loops. All these box contributions are calculated as in eqs. (93–95) in [39] and added directly to S_0 :

$$S_0 \rightarrow S_0 + x_t (\Delta_{H^\pm} + \Delta_{\chi_\pm}^q) \quad (3.3)$$

We have checked that at low $\tan\beta$, where the box contributions are most significant, the results in [10] are reproduced.

Double Penguin diagrams involving a neutral Higgs propagator connecting two flavor changing effective vertices can be significantly enhanced for large $\tan\beta$ or light scalars. We closely follow the analysis carried out in [37]:

- First, we compute flavor dependent ε parameters (effective vertices) arising from loops involving sparticles in the effective Lagrangian describing the Higgs quark couplings. We use Eq. (5.1) and appendix A.2 in [37]. However, we extend the neutralino sector according to the NMSSM; the corresponding generalization of the MSSM formulae is straightforward.
- Next, we define flavor-changing neutral Higgs-quark couplings $X_{LR/RL}^{Sbs}$ as in Eqs. (3.55–56) in [37] (S denote the various neutral Higgs bosons). The corresponding Higgs mixing angles x_d^S and x_u^S can be generalized in a straightforward way to the NMSSM using the decomposition of the neutral weak eigenstates H_u^0 and H_d^0 into the neutral physical states S^0 (in the convention of [37]) as $H_u^{0*} = \sum_{S^0} x_u^S S^0$, $H_d^0 = \sum_{S^0} x_d^S S^0$.
- Finally, we use Eq. (6.12) of [37] (neglecting the Goldstone boson contribution) for the three relevant coefficients C_1^{SLL} , C_1^{SRR} and C_2^{LR} . However, as we will face very light (pseudo)scalar masses (possibly below 10 GeV in some parts of the NMSSM parameter space), we can no longer be content with the approximation $\frac{1}{m_S^2}$ for the scalar propagator (see [17], Eq. (32)). Thus, we replace these factors by Breit-Wigner functions:

$$\frac{1}{m_S^2} \rightarrow \frac{\text{sgn}(m_S^2 - M_{B_q}^2)}{\sqrt{(m_S^2 - M_{B_q}^2)^2 + m_S^2 \Gamma_S^2}} \quad (3.4)$$

(The width Γ_S is computed as in NMSSMTools [46, 47].) In the MSSM, relations between the Higgs masses at large $\tan\beta$ allow for further simplifications of the final formula for ΔM_q (see [37], Eq. (6.23)). However, in the NMSSM a correct description of the singlet like contributions does not allow for such simplifications.

Next we consider $BR(\bar{B}_s \rightarrow \mu^+ \mu^-)$. We calculate the Branching Ratio according to Eq. (5.15-16) of [55] (we neglect the c'_i):

$$BR(\bar{B}_s \rightarrow \mu^+ \mu^-) = \frac{G_F^2 \alpha^2 M_{B_s}^5 f_{B_s}^2 \tau_{B_s}}{64\pi^3 \sin^4 \theta_W} |V_{tb} V_{ts}^*|^2 \sqrt{1 - 4 \frac{m_\mu^2}{m_{B_s}^2}} \left[\frac{1 - 4 \frac{m_\mu^2}{M_{B_s}^2}}{\left(1 + \frac{m_s}{m_b}\right)^2} |c_S|^2 + \left| \frac{c_P}{1 + \frac{m_s}{m_b}} + \frac{2m_\mu}{M_{B_s}^2} c_A \right|^2 \right] \quad (3.5)$$

where c_A contains the SM contribution arising from box and penguin diagrams, which is one order of magnitude below the sensitivity of present experimental data. The neutral Higgs contributions to c_S and c_P are the only ones which could lead to a significant deviation from the SM prediction. The corresponding diagrams involve the effective flavour violating neutral Higgs vertex and a neutral Higgs propagator. We infer from an appropriate generalization of the equations given in [37] the appropriate formulae for the coefficients c_S and c_P in the NMSSM. Again, it proves necessary to replace the approximation $\frac{1}{m_S^2}$ by a Breit-Wigner function.

Charged Higgs corrections to $BR(\bar{B}^+ \rightarrow \tau^+ \nu_\tau)$ were studied in [56] and lead to a destructive interference with the SM (W^+) contribution:

$$BR(\bar{B}^+ \rightarrow \tau^+ \nu_\tau) = \frac{G_F^2 M_B m_\tau^2}{8\pi} \left(1 - \frac{m_\tau^2}{M_B^2}\right)^2 f_B^2 |V_{ub}|^2 \tau_B r_H, \quad (3.6)$$

where r_H parametrizes the deviation from the SM prediction. The expression for r_H has been improved in [57] in order to take large $\tan\beta$ corrections into account:

$$r_H = \left[1 - \left(\frac{M_B}{m_{H^\pm}}\right)^2 \frac{\tan^2\beta}{1 + \tilde{\epsilon}_0 \tan\beta}\right]^2 \quad (3.7)$$

Having described the origin of all relevant calculations, we turn to the numerical results, concentrating first on $BR(\bar{B} \rightarrow X_s \gamma)$.

4 Results for $BR(\bar{B} \rightarrow X_s \gamma)$ in the MSSM and the NMSSM

The BSM contributions to $\bar{B} \rightarrow X_s \gamma$ depend essentially on the charged Higgs mass, $\tan\beta$ and, for large $\tan\beta$, on A_t .

First, we focus on the impact of the charged Higgs mass on $BR(\bar{B} \rightarrow X_s \gamma)$, which is always positive. The branching ratio is a decreasing function of m_{H^\pm} , since the contributions from charged Higgs diagrams decay like $1/m_{H^\pm}^4$. Before the recent improvements on the experimental side and the SM contributions discussed in the introduction, quite severe bounds on m_{H^\pm} could be deduced notably for small to modest values of $\tan\beta$, where the additional Susy contributions (which can have both signs, depending on the relative sign of A_t to μ) cannot be too large in absolute value.

The updated situation is described in Figs. 1–4. In Fig. 1 we show our results for $\bar{B} \rightarrow X_s \gamma$ for $\tan\beta = 5$, universal squark masses of 1 TeV, gaugino masses $M_1 = 150$ GeV,

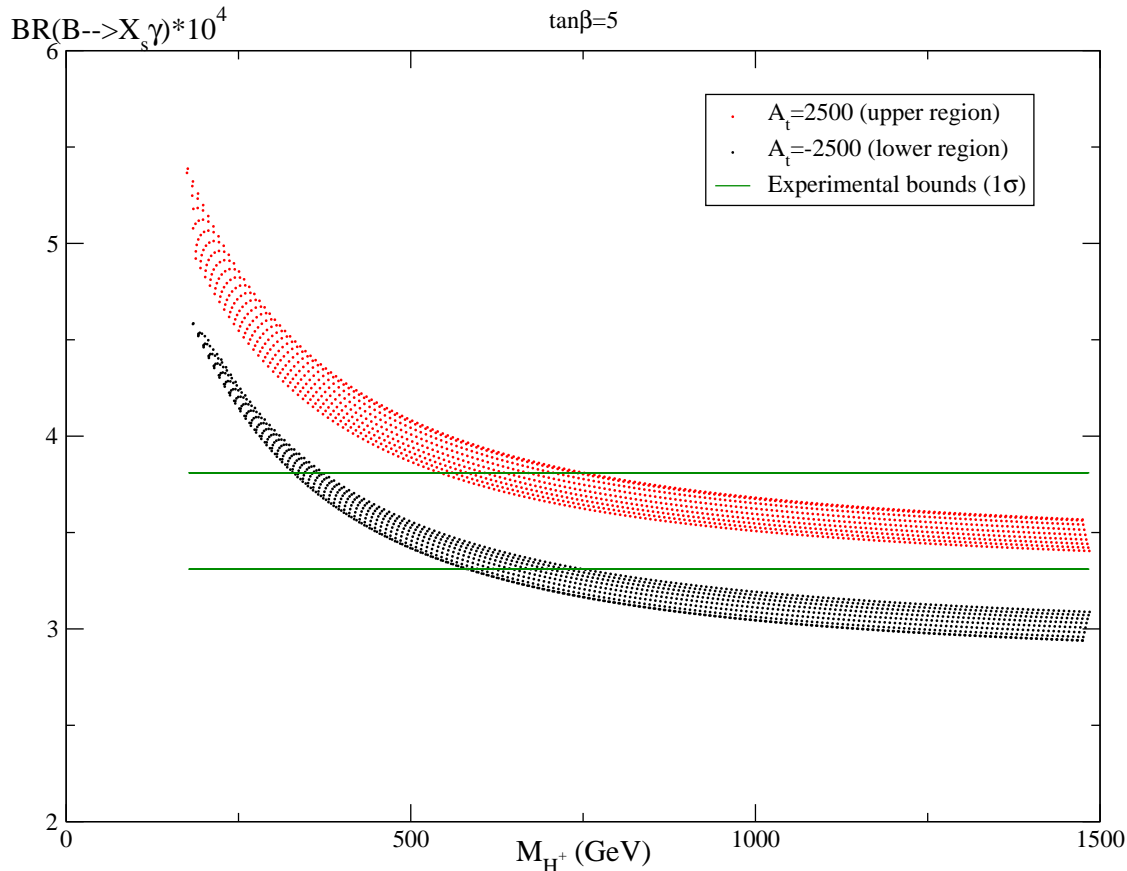


Figure 1: $BR(B \rightarrow X_s \gamma)$ as a function of the charged Higgs mass, for $\tan \beta = 5$, $A_t = \pm 2500$ GeV. The green lines represent the experimental 1σ bounds.

$M_2 = 300$ GeV, $M_3 = 900$ GeV, for two extreme values of $A_t = +2.5$ TeV and -2.5 TeV as a function of m_{H^\pm} . We scan over the parameter μ between $+100$ GeV and $+1$ TeV, which explains the broadening of the two dotted distributions. (The inner regions correspond to larger values of μ , the outer regions to the lowest value of μ that is allowed by the non-observation of charginos.) For the top quark mass we take 171.4 GeV. The 1σ experimentally allowed region is also indicated and it becomes clear that, at least after taking theoretical errors into account (see below), relatively low values of m_{H^\pm} down to ~ 200 GeV cannot be excluded. This result holds both for the MSSM and the NMSSM (where the μ -parameter has to be replaced by an effective parameter $\mu_{eff} = \lambda \langle S \rangle$, we use the conventions of [46]); no dependence on the additional parameters of the NMSSM remains visible.

Before we turn to larger values of $\tan \beta$, we study a relatively low value $\tan \beta = 2.2$ which would make it very difficult for the MSSM to satisfy the constraints from LEP on

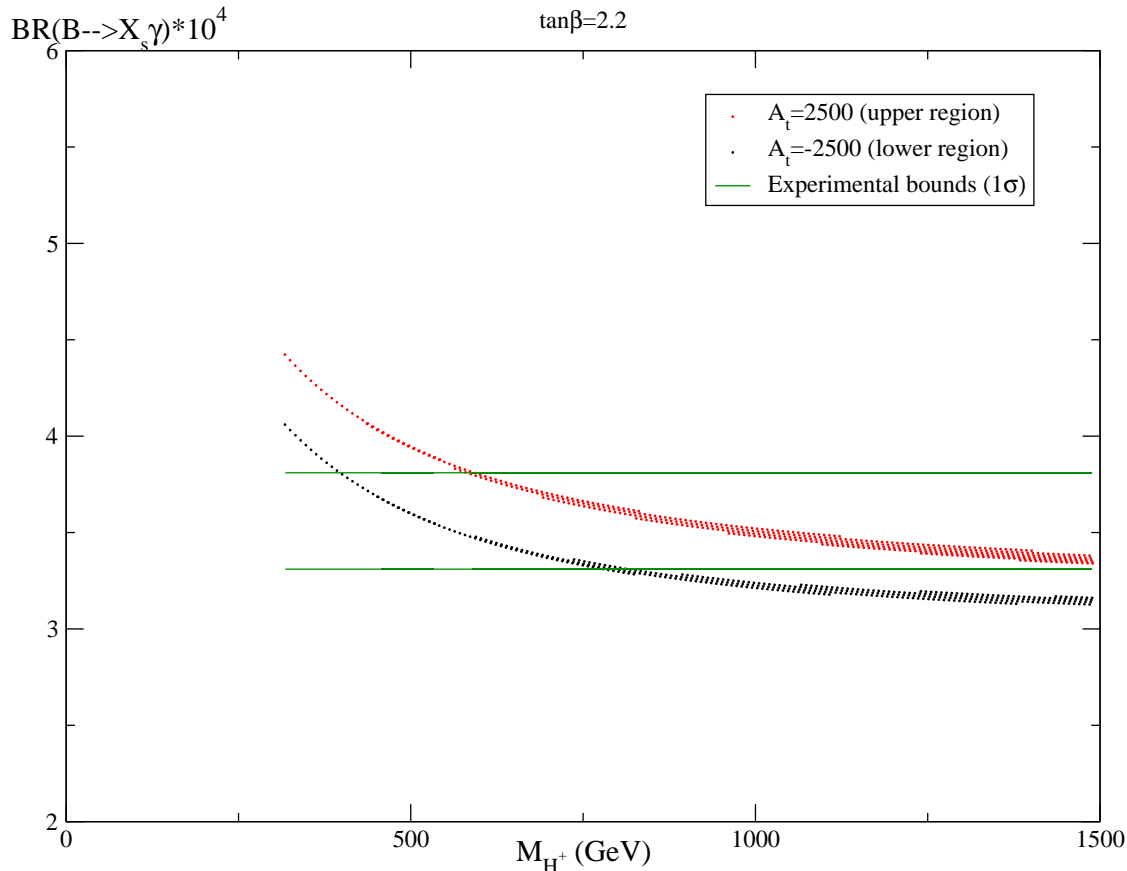


Figure 2: $BR(B \rightarrow X_s \gamma)$ as a function of the charged Higgs mass, for $\tan \beta = 2.2$, $A_t = \pm 2500$ GeV. The green lines represent the experimental 1σ bounds.

the lightest neutral Higgs boson mass, but which is perfectly consistent in the NMSSM [13], even in the CNMSSM with universal soft terms at the GUT scale [14]. Fig. 2 is the same as Fig. 1, but for $\tan \beta = 2.2$ and NMSSM parameters $\lambda = 0.5$, $\kappa = 0.4$ and $A_\kappa = -200$ GeV, which lead to neutral Higgs masses consistent with LEP bounds provided $m_{H^\pm} \gtrsim 300$ GeV (due to correlations between the various Higgs mass matrices in the NMSSM). There is no particular impact of the NMSSM parameters on $\bar{B} \rightarrow X_s \gamma$, however. One finds that this NMSSM specific region in parameter space is hardly constrained by this observable.

Next we investigate $\bar{B} \rightarrow X_s \gamma$ for larger values of $\tan \beta$. We find an approximate linear dependence on $\tan \beta$ with a slope determined essentially by A_t , at least for given μ , which we fix now at 300 GeV. In Fig. 3 we show our results for various values of A_t , $m_{H^\pm} = 300$ GeV (and the same other parameters as above), and in Fig. 4 for $m_{H^\pm} = 1$ TeV (which is obtained essentially by a vertical shift of Fig. 3). Now one finds that, the larger $\tan \beta$, the stronger

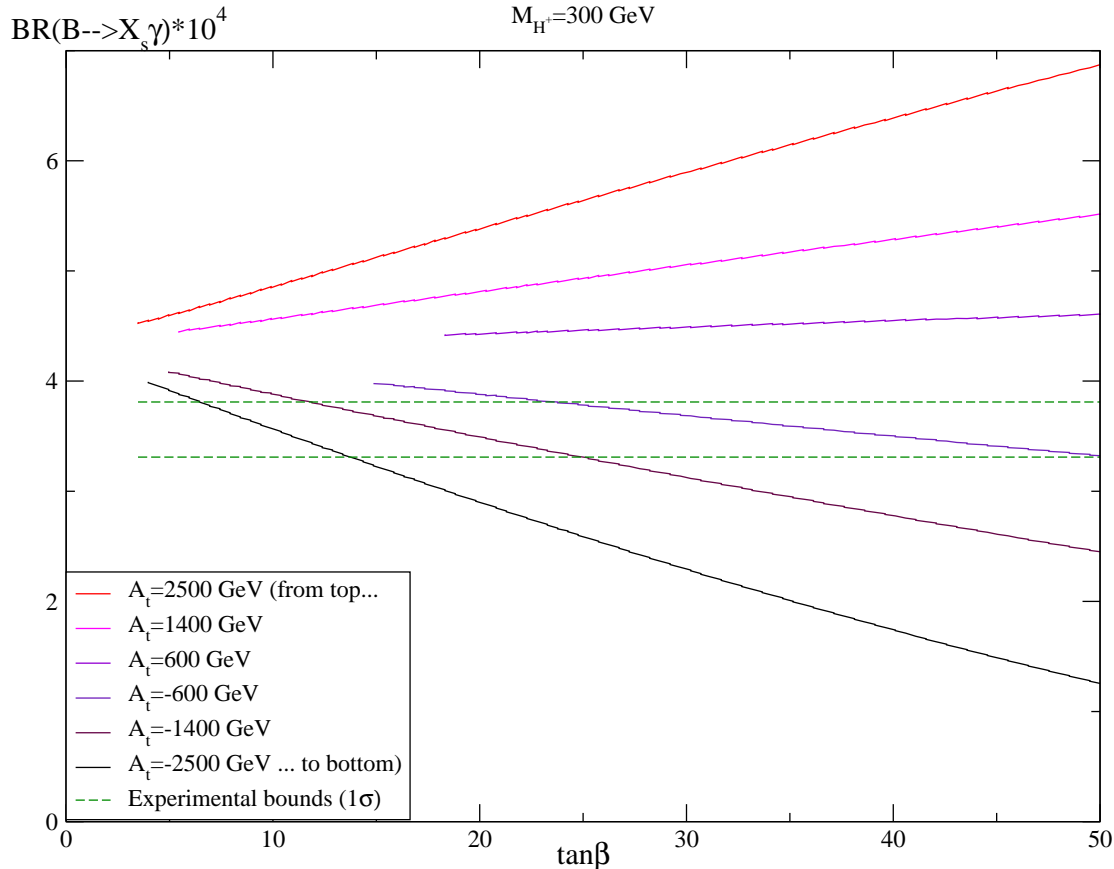


Figure 3: $BR(B \rightarrow X_s \gamma)$ as a function of $\tan \beta$, for $M_{H^+} = 300$ GeV and various values of A_t

are constraints on $|A_t|$ from $BR(\bar{B} \rightarrow X_s \gamma)$. On the other hand, positive contributions from relatively light charged Higgses can easily be cancelled by appropriate contributions from squark/chargino loops. Again, these results hold both for the MSSM and the NMSSM. We note that all points/lines shown in our Figures correspond to parameters which satisfy LEP constraints on Susy Higgs bosons, but this is not always trivial: small values of $|A_t|$ and $\tan \beta$ can lead to a too light neutral Higgs boson both in the MSSM and in the NMSSM; this is the reason why we confined ourselves to $|A_t| \geq 600$ GeV in Figs. 3 and 4, and why the lines (notably for $|A_t| = 600$ GeV) do not continue to arbitrarily small values of $\tan \beta$.

Although further dependencies on, e.g., the soft Susy breaking squark and gaugino masses would certainly merit further studies (which can be performed using NMSSMTools [23], once updated), we believe that our Figs. 1–4 represent a fairly comprehensive review of the actual status of the predictions for $BR(\bar{B} \rightarrow X_s \gamma)$ in the MSSM and the NMSSM.

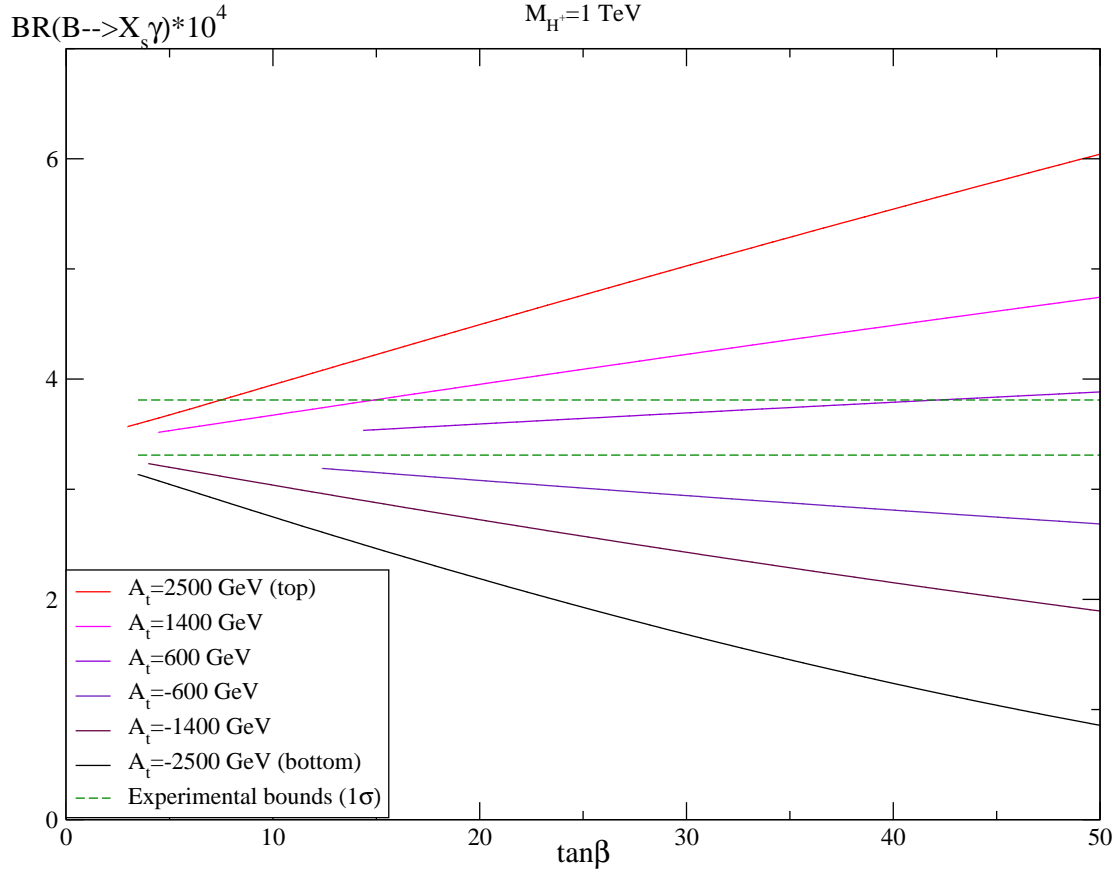


Figure 4: $BR(B \rightarrow X_s \gamma)$ as a function of $\tan \beta$, for $M_{H^+} = 1$ TeV and various values of A_t .

5 Constraints from $BR(\bar{B} \rightarrow X_s \gamma)$, $BR(\bar{B}_s \rightarrow \mu^+ \mu^-)$, ΔM_q , and $BR(\bar{B}^+ \rightarrow \tau^+ \nu_\tau)$ in the MSSM and the NMSSM

The aim of this chapter is to study the combination and the relative relevance of the constraints on the parameter space of the MSSM and the NMSSM from $BR(\bar{B} \rightarrow X_s \gamma)$, $BR(\bar{B}_s \rightarrow \mu^+ \mu^-)$, $\Delta M_{s,d}$ and $BR(\bar{B}^+ \rightarrow \tau^+ \nu_\tau)$. To this end we need to estimate the theoretical error implicit in our calculations. We intend to remain conservative and to denote a point as excluded only if one of the observables falls outside the 95% confidence limit (or 2σ).

In the case of $BR(\bar{B} \rightarrow X_s \gamma)$, the theoretical error will depend on the parameters of the Susy model under consideration; a general value for the theoretical error would be misleading. Hence we estimate the theoretical error separately for the charged Higgs, Susy and SM contributions to $BR(\bar{B} \rightarrow X_s \gamma)$ as follows: Since the charged Higgs contribution

is evaluated to NLO, we assume that its relative theoretical error is only 10%. For the Susy contribution, which is evaluated to LO only (up to leading logarithms), we assume a (conservative) relative theoretical error of 30%. Finally we estimate the theoretical error bars of the SM contribution as follows: Given that the improved treatment of the cut on the photon energy in [34] leads to a lower SM prediction than in [32], we allow the SM contribution to $BR(\bar{B} \rightarrow X_s \gamma)$ to vary in the range 2.72×10^{-4} to 3.38×10^{-4} . The SM and BSM errors are added linearly, which gives our estimate of the final theoretical error.

For ΔM_q and $BR(\bar{B}_s \rightarrow \mu^+ \mu^-)$, we estimate the theoretical error due to BSM contributions to be of the order of 30%, since no QCD corrections are taken into account. We add these uncertainties linearly to the 2σ SM error bars, which gives our complete theoretical error estimate. (The 1σ SM error bars on ΔM_q , arising mostly from the uncertainties of CKM matrix elements and lattice computations of hadronic parameters, are given in eqs. (1.5) and (1.7) above.)

Concerning $BR(\bar{B}^+ \rightarrow \tau^+ \nu_\tau)$, the uncertainties originating from the CKM matrix element $|V_{ub}|$ are considerable. We allow $|V_{ub}|$ to vary in the range $3.3 \times 10^{-3} \lesssim |V_{ub}| \lesssim 4.7 \times 10^{-3}$, with 4.0×10^{-3} as central value. For f_B we use $f_B = 0.216 \pm 0.022$ GeV as obtained by the HPQCD collaboration [58]. It just so happens that the corresponding central values lead to a SM prediction $BR(\bar{B}^+ \rightarrow \tau^+ \nu_\tau)|_{SM} = 1.32 \times 10^{-4}$ in agreement with the experimental central value given in (1.10). Allowing for 2σ error bars on f_B and the experimental average (1.10), and using the above range for $|V_{ub}|$ one finds that r_H in Eq. (3.7), neglecting additional theoretical errors, is allowed to vary over the quite large range

$$0.13 \lesssim r_H \lesssim 4.0 . \quad (5.1)$$

Consequently the constraints on the parameters $\tan \beta$ and m_{H^\pm} from this process are typically less stringent than the ones from other processes.

Now we turn to the dependence of the observables on the most relevant parameters.

ΔM_q and $BR(\bar{B}_s \rightarrow \mu^+ \mu^-)$ are quite sensitive to (double) Penguin contributions involving neutral Higgs bosons. These contributions are controlled by the parameter $\left(\frac{x_d^S \tan^\nu \beta}{m_S^2}\right)^2$, where $\nu = 3$ for $BR(\bar{B}_s \rightarrow \mu^+ \mu^-)$ and $\nu = 2$ for ΔM_q (and x_d^S denotes the H_d component of the neutral Higgs boson S); this explains why $BR(\bar{B}_s \rightarrow \mu^+ \mu^-)$ is usually more sensitive to neutral Higgs effects, at least at large $\tan \beta$ where they can become huge, leading to a violation of experimental bounds both in the MSSM and the NMSSM.

Thus, in general, large values of $\tan \beta$ are rather strongly constrained by these observables. However, it is still possible to reduce the neutral Higgs contributions by assuming heavy scalars and pseudoscalars (through a large doublet mass $M_A \sim M_{H^\pm}$). Another way to

circumvent these constraints consists in assuming parameters as the trilinear soft-coupling A_t or μ_{eff} such that the ε parameters (which control the flavour violating neutral Higgs couplings) remain small enough – here cancellations are often possible.

Only for low $\tan\beta$ can the positive contributions from Susy box diagrams to ΔM_s be more important than the double Penguin contributions. Given that the SM prediction for ΔM_s [36] is already $\sim 1\sigma$ above the CDF result [35], such additional positive BSM contributions could in principle exclude points in the parameter space at low $\tan\beta$. (For larger $\tan\beta$ the double Penguin diagram, which gives a negative contribution ΔM_q , usually dominates the box diagrams.) However, once we use 2σ error bars for the CKM matrix element and hadronic uncertainties, such exclusions at low $\tan\beta$ occur scarcely in practice.

In the following we present several examples of constraints on $\tan\beta$ and M_{H^\pm} (for fixed other parameters) that originate from the above processes.

First we consider the MSSM and the NMSSM for relatively small values of λ and κ ($\lesssim 0.1$), for which the contributions to the above processes are practically the same in both models. For the soft Susy breaking squark and gaugino masses we take the same values as in Figs. 1–4, and 300 GeV for μ (or μ_{eff} in the NMSSM).

In Fig. 5 we assume $A_t = 2.5$ TeV. Dark dotted regions are excluded by LEP: Here and in Figs. 6 and 7 below the non-observation of a light neutral Higgs scalar h at LEP implies lower limits on the MSSM parameter M_A (depending on $\tan\beta$ and A_t) which, in turn, lead to lower limits on M_{H^\pm} ($\sim M_A$ for large M_A). The domain allowed by LEP is further constrained by B physics processes. We note that the $BR(\bar{B} \rightarrow X_s \gamma)$ is by far the most stringent constraint in Fig. 5. It is indeed particularly severe because both the charged Higgs and the Susy contributions are positive and thus cannot balance each other. (Constraints from ΔM_d are never more restrictive than constraints from ΔM_s , hence ΔM_q in Figs. 5 and 6 stands for ΔM_s .)

In Fig. 6 we switch to $A_t = -2.5$ TeV, where the situation is quite different (the notation is the same as in Fig. 5): $BR(\bar{B} \rightarrow X_s \gamma)$ allows for additional domains, which originate from cancellations between the charged Higgs and Susy contributions (strongly enhanced by the large value of $|A_t|$). Therefore, light charged Higgs bosons (with masses down to ~ 100 GeV) are not excluded by this process; on the contrary, for $\tan\beta \gtrsim 20$, they must be light enough to avoid a large decrease of the branching ratio due to Susy diagrams. However, these regions are also constrained by $BR(\bar{B}_s \rightarrow \mu^+ \mu^-)$ and, less stringently, by $BR(\bar{B}^+ \rightarrow \tau^+ \nu_\tau)$ and ΔM_q .

In Fig. 7 we consider smaller values of $|A_t|$, $A_t = 600$ GeV: Now, small values of $\tan\beta$ and M_{H^\pm} (or M_A) are ruled out by LEP constraints on M_h . (The precise bound is very sensitive

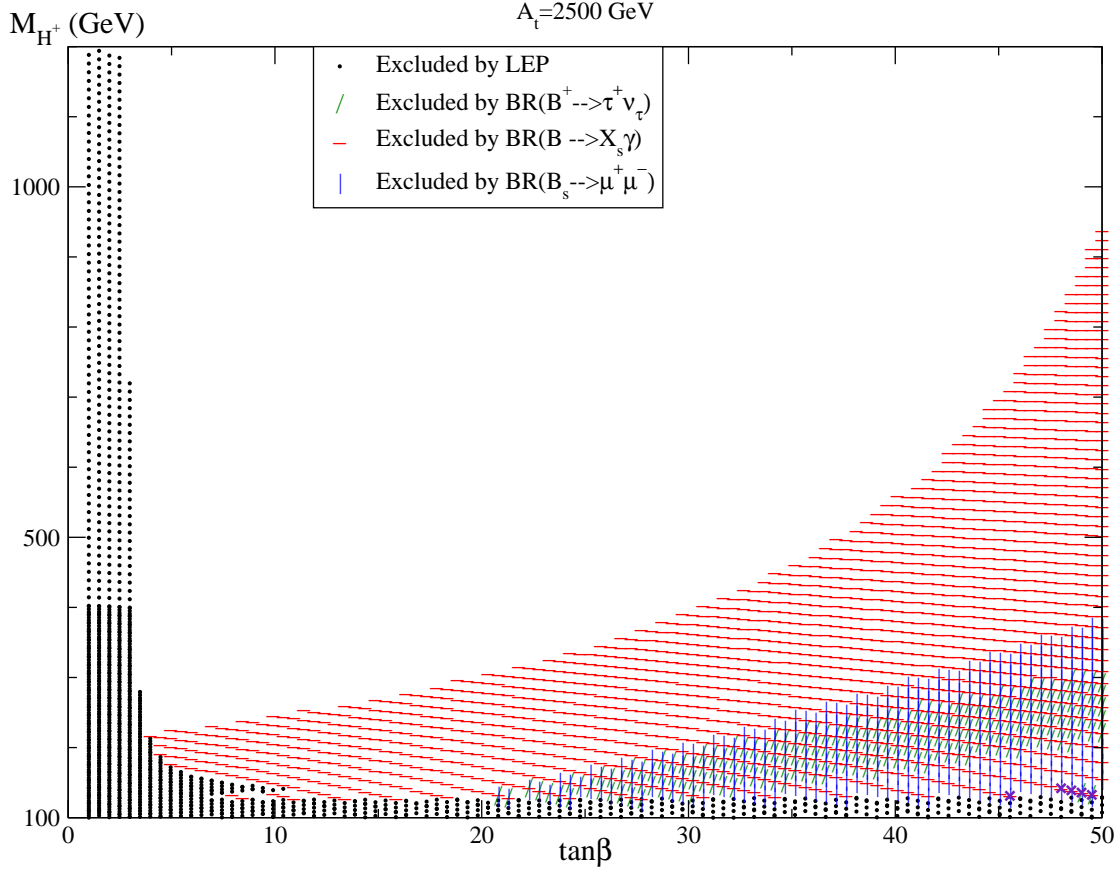


Figure 5: Constraints in the $\tan \beta - M_{H^+}$ plane for $A_t = 2500$ GeV.

to radiative corrections to M_h and hence to m_{top} . We recall that we use $m_{top} = 171.4$ GeV.) LEP constraints do not rule out a narrow strip around $M_{H^\pm} \sim 120$ GeV (already visible in Fig. 6), where the coupling of h to the Z-Boson is suppressed (since the MSSM-like parameter $\sin(\beta - \alpha)$ happens to be small) and where $M_h \sim 100$ GeV. However, even this region is now excluded by the charged Higgs contribution to $BR(\bar{B} \rightarrow X_s \gamma)$. (For positive or small absolute values of A_t the Susy contribution to $BR(\bar{B} \rightarrow X_s \gamma)$ cannot cancel the charged Higgs contribution.) $BR(\bar{B}_s \rightarrow \mu^+ \mu^-)$ does no longer lead to constraints since neutral Higgs effects, which are (roughly) proportional to A_t , remain small for a low value of this parameter. On the contrary, $BR(\bar{B}^+ \rightarrow \tau^+ \nu_\tau)$, which depends only weakly on A_t , can become the dominant B physics constraint for $\tan \beta \gtrsim 30$.

Next we discuss a region specific to the NMSSM: In the NMSSM, singlet-like pseudoscalars A_1 even below 10 GeV are able to survive LEP constraints. However, their loop induced flavour violating couplings to quarks and leptons can be large enough to cause sig-

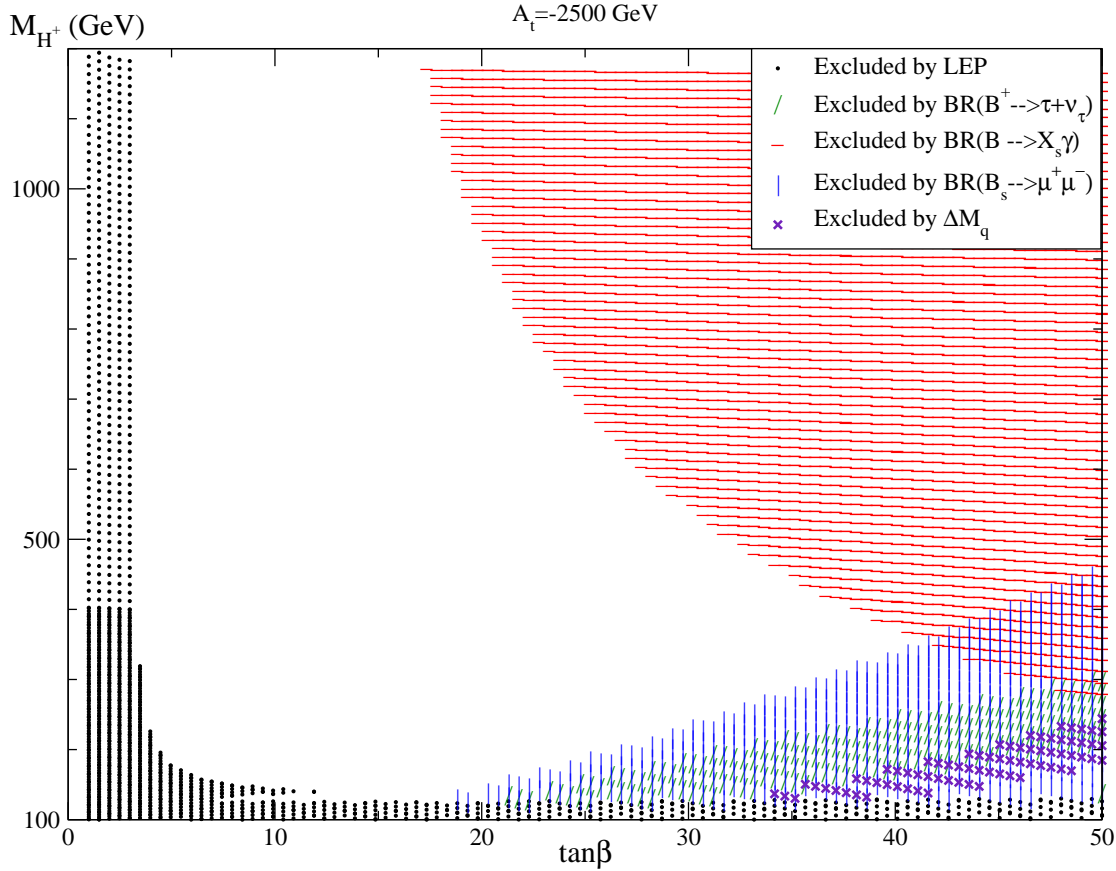


Figure 6: Constraints in the $\tan\beta$ - M_{H^+} plane for $A_t = -2500$ GeV.

nificant contributions to B physics observables, most of all for CP odd scalar masses near the resonance ($m_{A_1} \sim M_{B_q}$) and/or large $\tan\beta$. (Now, large values of $\tan\beta$ do not only lead to larger couplings of the light CP odd scalars, but also to an increase of their width which, in turn, enhances their contribution via the s-channel Penguin diagram even for masses a few GeV away from the resonance.)

In the following we present several examples of constraints on $\tan\beta$ and M_{A_1} that originate from B physics processes. For the soft Susy breaking squark and gaugino masses we take the same values as above, and 300 GeV for μ_{eff} . The NMSSM specific parameters are chosen as $\lambda = 0.45$, $\kappa = 0.4$ and $A_\kappa = -30$ GeV. However, A_λ (or the MSSM-like parameter $M_A^2 = \lambda S(A_\lambda + \kappa S)/(\cos\beta \sin\beta)$) must be chosen within a relatively narrow $\tan\beta$ -dependent window such that LEP constraints on all CP even and CP odd Higgs scalars remain satisfied. In Figs. 8–10 M_A is chosen within this ~ 1 –2 GeV wide window. (M_A varies from 300 to 400 GeV for $\tan\beta \sim 1.5$ to 10; LEP constraints would allow to extend this window up

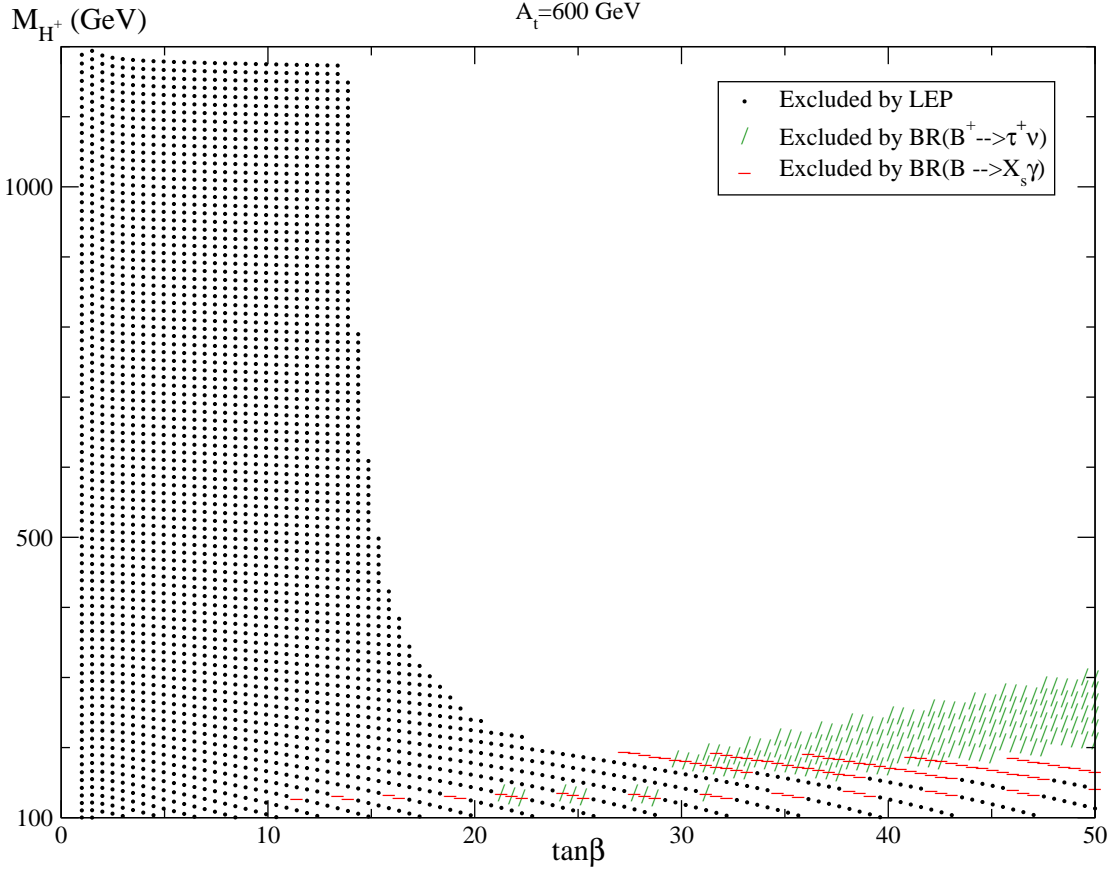


Figure 7: Constraints in the $\tan\beta$ - M_{H^+} plane for $A_t = 600$ GeV.

to $\tan\beta = 50$ with more finetuning on M_{A_1} ; however, B physics constraints exclude this domain.)

In Fig. 8 we consider the plane M_{A_1} vs. $\tan\beta$, and assume $A_t = -2.5$ TeV. Now, the constraints from $BR(\bar{B}_s \rightarrow \mu^+\mu^-)$ are the most relevant, and lead to strong upper limits on $\tan\beta$ at fixed M_{A_1} . Among the remaining observables, constraints from ΔM_s are also significant but generally redundant with the respect to $BR(\bar{B}_s \rightarrow \mu^+\mu^-)$.

Whereas the situation for $A_t = 2.5$ TeV in Fig. 9 is similar to the one with $A_t = -2.5$ TeV (the main difference comes from $BR(\bar{B} \rightarrow X_s\gamma)$, which excludes now a region with very light A_1 and $\tan\beta \gtrsim 7$ already covered by $BR(\bar{B}_s \rightarrow \mu^+\mu^-)$), the case $A_t = 500$ GeV considered in Fig. 10 is quite different: In contrast to Figs. 8 and 9 the lightest scalar Higgs mass m_h is below 90 GeV, but LEP constraints can still be satisfied due to the decay $h \rightarrow A_1A_1$.

Note that, on the one hand, A_1 in Fig. 10 has a $\sim 90\%$ singlet component, but also a $\sim 40\%$ doublet component. For $\tan\beta$ near 5 its coupling to down type quarks is even

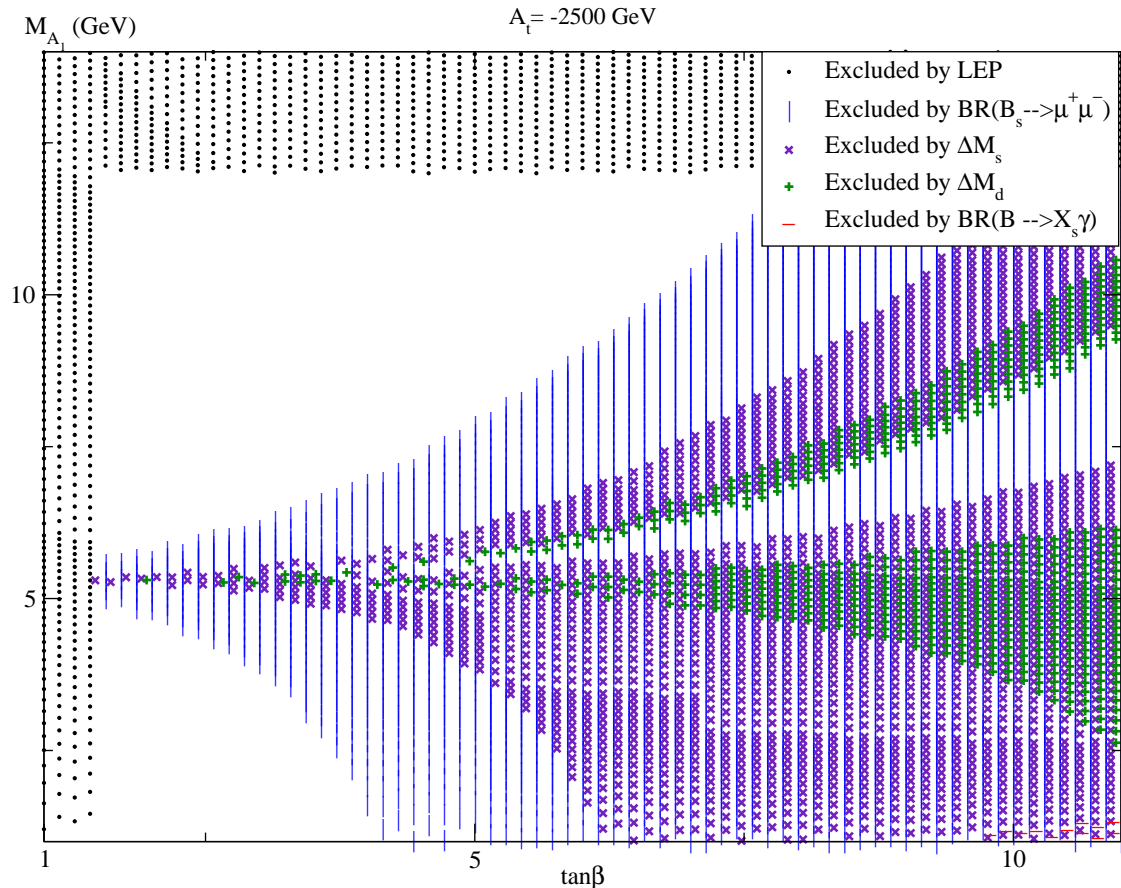


Figure 8: Constraints in the $\tan\beta$ - M_{A_1} plane for $A_t = -2500$ GeV.

~ 2 times larger than the one of a SM scalar Higgs boson. As function of M_{A_1} (and m_h), LEP constraints on $h \rightarrow A_1 A_1 \rightarrow 4 b$, $h \rightarrow A_1 A_1 \rightarrow 4 \tau$ or $h \rightarrow A_1 A_1 \rightarrow 4$ jets have then to be applied, which explains the jumps in the upper bound on $\tan\beta$. However, within the region allowed by LEP, B physics constraints are particularly weak: only a narrow stripe with M_{A_1} near $M_{\bar{B}_s}$ is excluded by $BR(\bar{B}_s \rightarrow \mu^+ \mu^-)$ and ΔM_s . Once again, this is due to the fact that neutral Higgs effects are essentially proportional to $|A_t|$ and small for small $|A_t|$.

6 Summary and Outlook

In this article, we have updated constraints from B physics observables on the parameters of the MSSM and the NMSSM (assuming minimal flavour violation), combining them with LEP constraints on the parameter space. Available SM and BSM radiative corrections are included in the calculations, which will be made public in the form of a Fortran code.

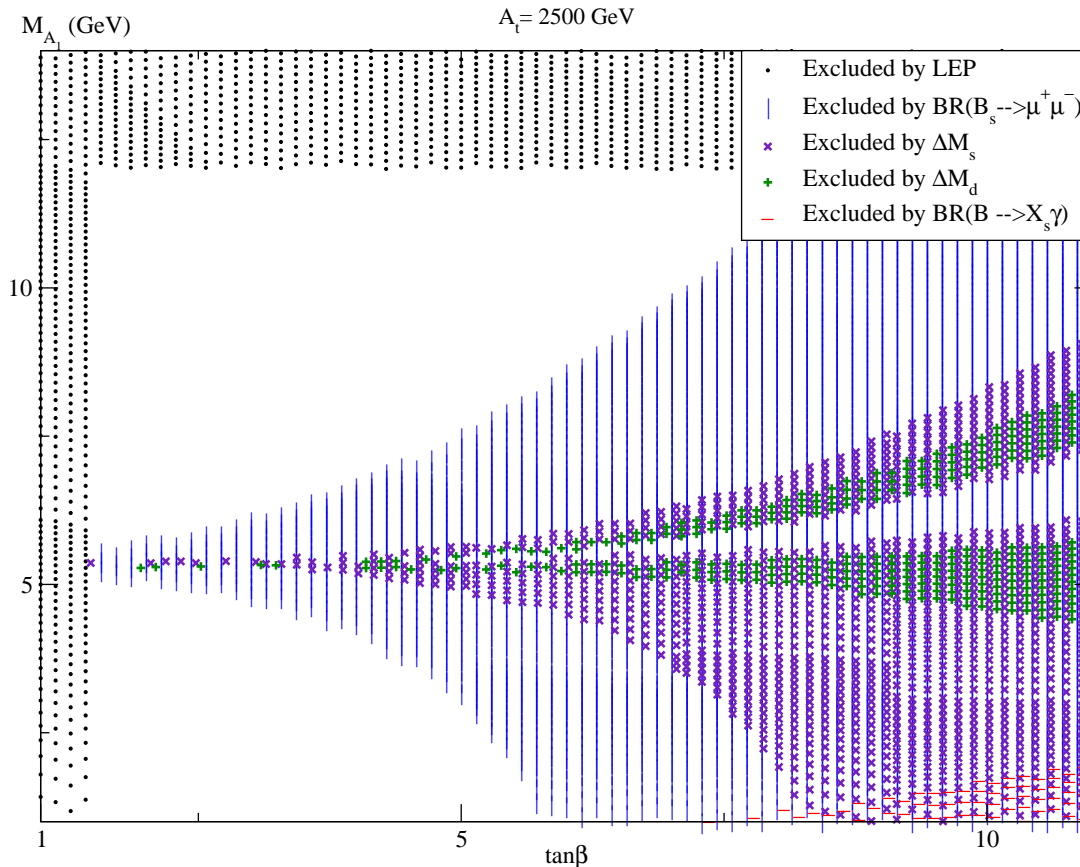


Figure 9: Constraints in the $\tan\beta$ - M_{A_1} plane for $A_t = 2500$ GeV.

As expected, constraints from $BR(\bar{B} \rightarrow X_s\gamma)$ have become weaker due to the recent increase of the world average, and the decrease of the SM prediction (which is now below the experimental average). Our numerical results (summarized in Figs. 1–4) show that constraints still arise if, simultaneously, M_{H^\pm} is small ($M_{H^\pm} \lesssim 300$ GeV) and $\tan\beta$ not too large ($\lesssim 10$), or if $\tan\beta \gtrsim 10$ and $|A_t|$ is large. We have verified explicitly (for the first time), that NMSSM specific contributions to $BR(\bar{B} \rightarrow X_s\gamma)$ are numerically negligible.

Among the other processes, $BR(\bar{B}_s \rightarrow \mu^+\mu^-)$ is typically the most sensitive and can exclude regions in parameter space for $\tan\beta \gtrsim 15$ that would be allowed by $BR(\bar{B} \rightarrow X_s\gamma)$, see Fig. 6. However, also $BR(\bar{B}^+ \rightarrow \tau^+\nu_\tau)$ can lead to the most relevant constraints for very large $\tan\beta$, cf. Fig. 7.

In the NMSSM specific case of a light CP odd Higgs scalar, constraints from $BR(\bar{B}_s \rightarrow \mu^+\mu^-)$ (inside the LEP allowed region) are quite strong for large $|A_t|$ (cf. Figs. 8 and 9), but exclude only a small region around $M_{A_1} \sim 5$ GeV for small $|A_t|$ (cf. Fig. 10).

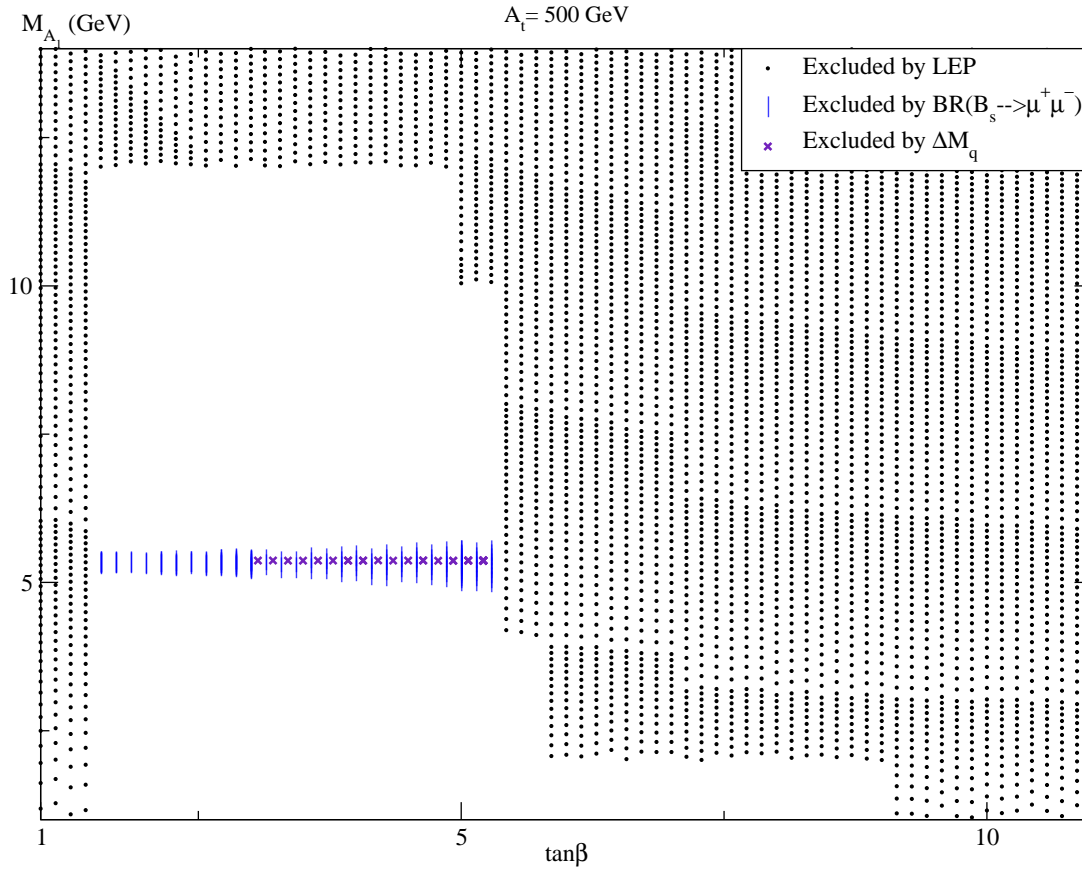


Figure 10: Constraints in the $\tan\beta$ - M_{A_1} plane for $A_t = 500$ GeV.

In the future, our calculations will allow to combine constraints from B physics observables with additional assumptions such as universal soft terms at the GUT scale (the CMSSM and the CNMSSM) and/or constraints from the dark matter relic density via NMSSM-Tools [23].

References

- [1] M. S. Carena, A. Menon, R. Noriega-Papaqui, A. Szyrkman and C. E. M. Wagner, Phys. Rev. D **74** (2006) 015009 [arXiv:hep-ph/0603106].
- [2] M. Carena, A. Menon and C. E. M. Wagner, Phys. Rev. D **76** (2007) 035004 [arXiv:0704.1143 [hep-ph]].
- [3] G. Isidori and P. Paradisi, Phys. Lett. B **639** (2006) 499 [arXiv:hep-ph/0605012].
- [4] J. Ellis, S. Heinemeyer, K. A. Olive, A. M. Weber and G. Weiglein, “The Supersymmetric Parameter Space in Light of B-physics Observables and Electroweak Precision Data,” arXiv:0706.0652 [hep-ph].
- [5] M. Blanke, A. J. Buras, D. Guadagnoli and C. Tarantino, JHEP **0610** (2006) 003 [arXiv:hep-ph/0604057].
- [6] P. Ball and R. Fleischer, Eur. Phys. J. C **48** (2006) 413 [arXiv:hep-ph/0604249].
- [7] M. Blanke and A. J. Buras, JHEP **0705** (2007) 061 [arXiv:hep-ph/0610037].
- [8] A. Freitas, E. Gasser and U. Haisch, Phys. Rev. D **76** (2007) 014016 [arXiv:hep-ph/0702267].
- [9] G. Isidori, F. Mescia, P. Paradisi and D. Temes, Phys. Rev. D **75** (2007) 115019 [arXiv:hep-ph/0703035].
- [10] W. Altmannshofer, A. J. Buras and D. Guadagnoli, “The MFV limit of the MSSM for low $\tan(\beta)$: meson mixings revisited,” arXiv:hep-ph/0703200.
- [11] D. G. Cerdeno, E. Gabrielli, D. E. Lopez-Fogliani, C. Munoz and A. M. Teixeira, JCAP **0706** (2007) 008 [arXiv:hep-ph/0701271].
- [12] C. Hugonie, G. Belanger and A. Pukhov, “Dark Matter in the Constrained NMSSM,” arXiv:0707.0628 [hep-ph].
- [13] U. Ellwanger and C. Hugonie, Mod. Phys. Lett. A **22** (2007) 1581 [arXiv:hep-ph/0612133].
- [14] U. Ellwanger and C. Hugonie, Comput. Phys. Commun. **177** (2007) 399 [arXiv:hep-ph/0612134].

- [15] B. A. Dobrescu, G. Landsberg and K. T. Matchev, Phys. Rev. D **63** (2001) 075003 [arXiv:hep-ph/0005308].
- [16] B. A. Dobrescu and K. T. Matchev, JHEP **0009** (2000) 031 [arXiv:hep-ph/0008192].
- [17] G. Hiller, Phys. Rev. D **70** (2004) 034018 [arXiv:hep-ph/0404220].
- [18] R. Dermisek and J. F. Gunion, Phys. Rev. Lett. **95** (2005) 041801 [arXiv:hep-ph/0502105], Phys. Rev. D **73** (2006) 111701 [arXiv:hep-ph/0510322], Phys. Rev. D **75** (2007) 075019 [arXiv:hep-ph/0611142], and arXiv:0705.4387.
- [19] U. Ellwanger, J. F. Gunion and C. Hugonie, JHEP **0507** (2005) 041 [arXiv:hep-ph/0503203].
- [20] S. Moretti, S. Munir and P. Poulose, Phys. Lett. B **644** (2007) 241 [arXiv:hep-ph/0608233].
- [21] K. Cheung, J. Song and Q. S. Yan, Phys. Rev. Lett. **99** (2007) 031801 [arXiv:hep-ph/0703149], “Roles of Higgs decay into two pseudoscalar bosons in the search of intermediate-mass Higgs Boson,” arXiv:0710.1997 [hep-ph].
- [22] M. A. Sanchis-Lozano, “A light non-standard Higgs boson: to be or not to be at a (Super) B factory?”, arXiv:0709.3647 [hep-ph].
- [23] see: www.th.u-psud.fr/NMHDECAY/nmssmtools.html
- [24] S. Heinemeyer, W. Hollik and G. Weiglein, Comput. Phys. Commun. **124** (2000) 76 [arXiv:hep-ph/9812320], G. Degrassi, S. Heinemeyer, W. Hollik, P. Slavich and G. Weiglein, Eur. Phys. J. C **28** (2003) 133 [arXiv:hep-ph/0212020], see: www.feynhiggs.de
- [25] A. Djouadi, J. L. Kneur and G. Moultaka, Comput. Phys. Commun. **176** (2007) 426 [arXiv:hep-ph/0211331].
- [26] G. Belanger, F. Boudjema, A. Pukhov and A. Semenov, Comput. Phys. Commun. **149** (2002) 103 [arXiv:hep-ph/0112278].
- [27] G. Belanger, F. Boudjema, A. Pukhov and A. Semenov, Comput. Phys. Commun. **174** (2006) 577 [arXiv:hep-ph/0405253].
- [28] W. Porod, Comput. Phys. Commun. **153** (2003) 275 [arXiv:hep-ph/0301101].

- [29] P. Gambino and M. Misiak, Nucl. Phys. B **611** (2001) 338 [arXiv:hep-ph/0104034].
- [30] T. Hurth, E. Lunghi and W. Porod, Nucl. Phys. B **704** (2005) 56 [arXiv:hep-ph/0312260].
- [31] E. Barberio *et al.* [Heavy Flavor Averaging Group (HFAG)], “Averages of b-hadron properties at the end of 2005,” arXiv:hep-ex/0603003, and www.slac.stanford.edu/xorg/hfag.
- [32] M. Misiak *et al.*, Phys. Rev. Lett. **98** (2007) 022002 [arXiv:hep-ph/0609232].
- [33] M. Misiak and M. Steinhauser, Nucl. Phys. B **764** (2007) 62 [arXiv:hep-ph/0609241].
- [34] T. Becher and M. Neubert, Phys. Rev. Lett. **98** (2007) 022003 [arXiv:hep-ph/0610067].
- [35] A. Abulencia *et al.* [CDF Collaboration], Phys. Rev. Lett. **97** (2006) 242003 [arXiv:hep-ex/0609040].
- [36] E. Dalgic *et al.*, Phys. Rev. D **76** (2007) 011501 [arXiv:hep-lat/0610104].
- [37] A. J. Buras, P. H. Chankowski, J. Rosiek and L. Slawianowska, Nucl. Phys. B **659** (2003) 3 [arXiv:hep-ph/0210145].
- [38] M. Okamoto, “Full determination of the CKM matrix using recent results from lattice QCD,” PoS **LAT2005** (2006) 013 [arXiv:hep-lat/0510113].
- [39] S. Bertolini, F. Borzumati, A. Masiero and G. Ridolfi, Nucl. Phys. B **353** (1991) 591.
- [40] CDF Collaboration, “Search for $B_s^0 \rightarrow \mu^+\mu^-$ and $B_d^0 \rightarrow \mu^+\mu^-$ Decays in 2 fb^{-1} of $p\bar{p}$ Collisions with CDF II”, CDF Public Note 8956 (2007)
- [41] G. Buchalla, A. J. Buras and M. E. Lautenbacher, Rev. Mod. Phys. **68** (1996) 1125 [arXiv:hep-ph/9512380].
- [42] A. Dedes, H. K. Dreiner, U. Nierste and P. Richardson, arXiv:hep-ph/0207026.
- [43] K. Ikado *et al.* [Belle Collaboration], Phys.Rev.Lett.**97:251802** (2006) [arXiv:hep-ex/0604018].
- [44] B. Aubert *et al.* [BABAR Collaboration], arXiv:hep-ex/0608019.
- [45] M. Bona *et al.* [UTfit Collaboration], JHEP **0610** (2006) 081 [arXiv:hep-ph/0606167].

- [46] U. Ellwanger, J. F. Gunion and C. Hugonie, *JHEP* **0502** (2005) 066 [arXiv:hep-ph/0406215].
- [47] U. Ellwanger and C. Hugonie, *Comput. Phys. Commun.* **175** (2006) 290 [arXiv:hep-ph/0508022].
- [48] P. Gambino and U. Haisch, *JHEP* **0110** (2001) 020 [arXiv:hep-ph/0109058].
- [49] G. Degrassi, P. Gambino and G. F. Giudice, *JHEP* **0012** (2000) 009 [arXiv:hep-ph/0009337].
- [50] M. Carena, D. Garcia, U. Nierste and C. E. M. Wagner, *Nucl. Phys. B* **577** (2000) 88 [arXiv:hep-ph/9912516]; *Phys. Lett. B* **499** (2001) 141 [arXiv:hep-ph/0010003].
- [51] M. Ciuchini, G. Degrassi, P. Gambino and G. F. Giudice, *Nucl. Phys. B* **534** (1998) 3 [arXiv:hep-ph/9806308].
- [52] G. Degrassi, P. Gambino and P. Slavich, *Phys. Lett. B* **635** (2006) 335 [arXiv:hep-ph/0601135].
- [53] M. Ciuchini, G. Degrassi, P. Gambino and G. F. Giudice, *Nucl. Phys. B* **527** (1998) 21 [arXiv:hep-ph/9710335].
- [54] G. D'Ambrosio, G. F. Giudice, G. Isidori and A. Strumia, *Nucl. Phys. B* **645** (2002) 155 [arXiv:hep-ph/0207036].
- [55] C. Bobeth, A. J. Buras, F. Kruger and J. Urban, *Nucl. Phys. B* **630** (2002) 87 [arXiv:hep-ph/0112305].
- [56] W. S. Hou, *Phys. Rev. D* **48** (1993) 2342.
- [57] A. G. Akeroyd and S. Recksiegel, *J. Phys. G* **29** (2003) 2311 [arXiv:hep-ph/0306037].
- [58] A. Gray *et al.* [HPQCD Collaboration], *Phys. Rev. Lett.* **95** (2005) 212001 [arXiv:hep-lat/0507015].